Liquid Crystals
Publication details, including instructions for authors and subscription information:
http://www.informaworld.com/smpp/title~content=t713926090

Perturbation theory for nematic liquid crystals of axially symmetric molecules: Numerical results at high pressures including second- and fourth rank orientational order parameters

Kalyan Singh[a]; U. P. Singh[a]
[a] Department of Physics and Electronics, Avadh University Faizabad (U.P.), India

To cite this Article Singh, Kalyan and Singh, U. P.(1989) 'Perturbation theory for nematic liquid crystals of axially symmetric molecules: Numerical results at high pressures including second- and fourth rank orientational order parameters', Liquid Crystals, 6: 6, 641 — 655
To link to this Article: DOI: 10.1080/02678298908029107
URL: http://dx.doi.org/10.1080/02678298908029107

LIQUID CRYSTALS, 1989, VOL. 6, NO. 6, 641–655

Perturbation theory for nematic liquid crystals of axially symmetric molecules: Numerical results at high pressures including second- and fourth rank orientational order parameters

by KALYAN SINGH and U. P. SINGH

Department of Physics and Electronics, Avadh University Faizabad (U.P.) 224001, India

(*Received 9 September 1988; accepted 28 June 1989*)

A statistical mechanical perturbation theory is applied to study the thermodynamic properties of nematic liquid crystals at the nematic–isotropic (N–I) phase transition under pressure, retaining second- and fourth-rank long-range orientational order parameters. We report calculations for a hard ellipsoidal system superposed with an attractive interaction and subjected to different external pressures. The repulsive interaction is represented by a repulsion between hard ellipsoids characterized by a length-to-width ratio and the interaction arising from the dispersion interaction between two asymmetric molecules represents the attractive interaction. The inclusion of the fourth-rank order parameter in the effective one-body potential $\psi(\Omega)$ does not lead to a significant overall improvement. The influence of pressure on the stability, ordering and thermodynamic functions at the N–I transition is analysed. We find that our theoretical predictions are in accordance with experimental observations.

1. Introduction

Systems composed of nonspherical molecules exhibit a variety of phases ranging from orientationally ordered crystals to orientationally disordered crystals and mesophases. A simple theoretical model for nonspherical molecules is a hard-ellipsoid system. Frenkel and Mulder [1] have discovered four distinct phases, viz. isotropic fluid, nematic fluid, ordered solid and plastic solid, by Monte Carlo simulation of hard ellipsoids. A system consisting of hard ellipsoids is also a good reference system for perturbation theories of molecular fluids. There have been a number of attempts [2–7] in the recent past to study the orientational ordering and thermodynamic quantities in liquid crystals at high pressures.

In a previous paper, Singh and Singh [8] (referred to as I) developed a statistical mechanical perturbation theory to describe the equilibrium properties of nematic liquid crystals. The theory, like the van der Waals theories, is based on the assumption that the predominant factor in determining liquid crystalline stability is geometric. Thermodynamic properties were calculated for a trial system composed of molecules interacting via a pair potential having both repulsive and attractive parts. The attractive potential a function of only the centre of mass distance and the relative orientation between the two molecules, was approximated by the interaction arising from the dispersion interaction between two asymmetric molecules.

Singh and Singh [9] (referred to as II) have extended the theory of I to analyse the thermodynamic and orientational behaviour of nematogens close to the N–I phase transition under high pressure. They have also investigated the effect of quadrupolar interactions [10] on the stability and ordering of the nematic phase under high pressure. But in all calculations reported by Singh and Singh [8–10] their investigation was limited in the sense that only the second-rank order parameter was taken into consideration. However, experimentally, the importance of both second- and fourth-rank order parameters (S_2, S_4) has been demonstrated [11].

In the present paper, we refine our calculation of II by retaining both second- and fourth-rank long-range orientational order terms in the evaluation of the angle-dependent term in the expression for the excluded volume and the perturbation term under high pressure. We report our results for the thermodymnamic properties at the N–I transition for a system of hard ellipsoids (characterized by length-to-width ratio x_0) superposed with an attractive potential described by a dispersion interaction at various pressures ranging from 1 bar to 500 bar. A brief account of the perturbation method and the working equations are given in the following section. Results and discussions are presented in §3.

2. Perturbation theory

The perturbation expansion method used is entirely the same as outlined in I. We consider a system composed of N axially symmetric nonspherical nematogenic molecules contained in a volume V at temperature T, which interact pairwise through the potential defined by

$$u_N(\mathbf{x}_1, \mathbf{x}_2, \ldots, \mathbf{x}_N) = \sum_{1 \leq i < j \leq N} u_0(\mathbf{x}_i, \mathbf{x}_j) + \sum_{1 \leq i < j \leq N} u_p(\mathbf{x}_i, \mathbf{x}_j), \tag{1}$$

where the vector $\mathbf{x}_i = (\mathbf{r}_i, \Omega_i)$ represents both the position of the centre of mass and the orientation of the ith molecule. u_0 represents the reference potential and is described by the repulsion between hard ellipsoids of length $2a$ and width $2b$ and length-to-width ratio $x_0(=a/b)$. $u_0 = \infty$ for any $\mathbf{r}_{12}$, Ω_1, Ω_2 such that the rods 1 and 2 overlap and equals zero otherwise. u_p is the perturbation potential which is defined as the more smoothly varying long-range attractive part.

Following the statistical mechanical machinery as outlined in I, the perturbation series for the Helmholtz free energy is written as

$$\frac{\beta A}{N} = \frac{\beta A_0}{N} + \sum_{s=1}^{\infty} \frac{\beta A^{(s)}}{N}, \tag{2}$$

where A_0 is the reference system contribution to A and

$$\frac{\beta A^{(s)}}{N} = \beta \int f(\Omega_1) d\Omega_1 \psi^{(s)}(\Omega_1) \tag{3}$$

represents the perturbation terms. s denotes the order of the perturbation. $\beta = 1/kT$ with k the Boltzmann constant. $\psi(\Omega_1)$ is defined as the effective one-body orientational perturbation potential given by the relation

$$\psi^{(s)}(\Omega_1) = \frac{1}{2s} \varrho \int d\Omega_2 f(\Omega_2) \int d\mathbf{r}_{12} u_p(\mathbf{r}_{12}, \Omega_1, \Omega_2)\, g^{(s-1)}(\mathbf{r}_{12}, \Omega_1, \Omega_2), \tag{4}$$

where $g^{(0)}(\mathbf{r}_{12}, \Omega_1, \Omega_2)$ is the pair correlation function (PCF) for the reference system. Other symbols have their usual meanings. In our present development we need to know only $\tilde{g}^{(0)}(\mathbf{r}_{12}, \Omega_{12})$ which is defined as (as explained in I)

$$\tilde{g}^{(0)}(\mathbf{r}_{12}, \Omega_{12}) = \int d\hat{\mathbf{r}}_{12}\, g^{(0)}(\hat{\mathbf{r}}_{12}, \Omega_1, \Omega_2),$$

where $\hat{\mathbf{r}}_{12}$ is a unit vector along the axis joining the centres of two ellipsoids.

2.1. *Reference system*

For estimating the thermodynamic properties of a system of hard ellipsoids, we start with the pressure equation

$$\frac{\beta p_0}{\varrho} = 1 - \tfrac{1}{6}\beta\varrho \int d\mathbf{r}_{12} \int f(\Omega_1)d\Omega_1 \int f(\Omega_2)d\Omega_2\, [\mathbf{r}_{12}\nabla u_0(\mathbf{r}_{12}, \Omega_{12})]\tilde{g}^{(0)}(\mathbf{r}_{12}, \Omega_{12}) \tag{5}$$

where the operator ∇ acts only on the $\mathbf{r}_{12}$ coordinates of $u_0(\mathbf{r}_{12}, \Omega_{12})$. The hard ellipsoid potential satisfies the relation

$$\begin{aligned} u_0(\mathbf{r}_{12}, \Omega_{12}) &= u_0[\mathbf{r}_{12}/D(\mathbf{r}_{12}, \Omega_{12})], \\ &= u_0(r_{12}^*) = \begin{cases} \infty & \text{for } r_{12}^* < 1, \\ 0 & \text{for } r_{12}^* > 1, \end{cases} \end{aligned} \tag{6}$$

where $D(\mathbf{r}_{12}, \Omega_{12})$ is the distance of closest approach of two molecules with relative orientation Ω_{12}. Following the Berne and Pechukas [12] gaussian overlap model, we approximate the distance of closest approach $D(\Omega_{12})[\equiv D(\mathbf{r}_{12}, \Omega_{12})]$ by the relation

$$D(\hat{\mathbf{r}}_{12}, \Omega_{12}) = D_0\left[1 - \chi\frac{(\hat{\mathbf{r}}_{12}\cdot\hat{\mathbf{e}}_1)^2 + (\hat{\mathbf{r}}_{12}\cdot\hat{\mathbf{e}}_2)^2 - 2\chi(\hat{\mathbf{r}}_{12}\cdot\hat{\mathbf{e}}_1)(\mathbf{r}_{12}\cdot\hat{\mathbf{e}}_2)(\hat{\mathbf{e}}_1\cdot\hat{\mathbf{e}}_2)}{1 - \chi^2(\hat{\mathbf{e}}_1\cdot\hat{\mathbf{e}}_2)^2}\right]^{-1/2} \tag{7}$$

which is a reasonably good approximation to the distance of closest approach of two hard ellipsoids rather than of two hard spherocylinders as assumed by Singh and Singh [8–10]. $D_0(=2b)$ is the length of the minor axis. $\hat{\mathbf{e}}_1$ and $\hat{\mathbf{e}}_2$ are unit vectors along the symmetry axes of two interacting ellipsoids of length-to-width ratio x_0 and

$$\chi = (x_0^2 - 1)/(x_0^2 + 1). \tag{8}$$

Equation (5) involves the hard-ellipsoid pair correlation function which is related to the probability of finding a hard ellipsoid with known orientation at a given distance from the reference hard ellipsoid whose position and orientation are known. Following Parsons [13] and using decoupling approximation, we assume that $\tilde{g}^{(0)}(\mathbf{r}_{12}, \Omega_{12})$ scales as $g^{(0)}[r_{12}/D(\Omega_{12})]$, which decouples the orientational degrees of freedom from the translational ones to all orders in the density, i.e.

$$\tilde{g}^{(0)}(\mathbf{r}_{12}, \Omega_{12}) = g^{(0)}[r_{12}/D(\Omega_{12})] = g_{\text{hs}}^{(0)}(r_{12}^*). \tag{9}$$

With the help of equation (9) equation (5) reduces to

$$\frac{\beta p_0}{\varrho} = 1 + \tfrac{1}{2}\varrho g_{\text{hs}}^{(1)} \langle V_{\text{exc}}(\Omega_{12})\rangle\, \Omega_1, \Omega_2 \tag{10}$$

where the angular bracket $\langle\cdot\cdot\cdot\rangle$ denotes the ensemble average over the remaining $N - 2$ particles of the system. $g_{\text{hs}}^{(1)}$ is the value of the radial distribution function of two hard spheres at contact and $V_{\text{exc}}(\Omega_{12})$ is the excluded volume or co-volume

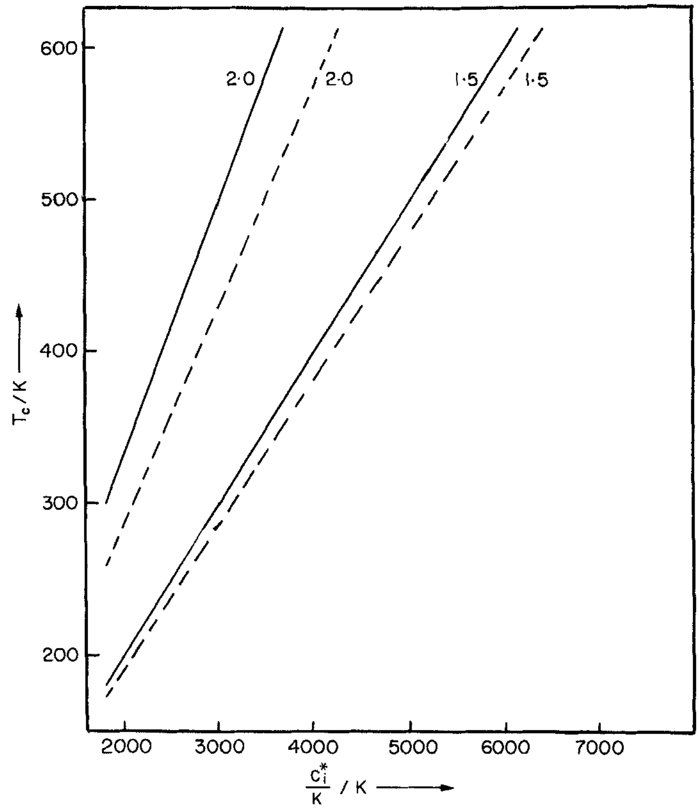

Figure 1. The variation of N–I transition temperature T_c as a function of C_i^*/k (K) for a fixed value of $C_i^*/C_a^* = 20$. The numbers on the curves indicate the value of x_0. Dashed and solid lines correspond, respectively, to pressure 1 bar and 300 bar.

between the two ellipsoids. $V_{\text{exc}}(\Omega_{12})$ is given by [13]

$$V_{\text{exc}}(\Omega_{12}) = \frac{1}{3}\int D^3(\hat{\mathbf{r}}_{12}, \Omega_{12})\, d\hat{\mathbf{r}}_{12}. \tag{11}$$

Performing this integration for fixed relative orientation $\hat{\mathbf{e}}_1 \cdot \hat{\mathbf{e}}_2 = \cos\theta_{12}$ we get

$$V_{\text{exc}}(\Omega_{12}) = 8V_0(1 - \chi^2)^{-1/2}(1 - \chi^2\cos^2\theta_{12})^{1/2}, \tag{12}$$

where V_0 is the volume of an ellipsoid. Expanding equation (12) in powers of $\chi^2\cos^2\theta_{12}$, we get

$$\begin{aligned}\langle V_{\text{exc}}(\Omega_{12})\rangle = {} & 8V_0(1 - \chi^2)^{-1/2}(1 - \tfrac{1}{2}\chi^2\langle\cos^2\theta_{12}\rangle_{\Omega_1,\Omega_2} - \tfrac{1}{8}\chi^4\langle\cos^4\theta_{12}\rangle_{\Omega_1,\Omega_2} \\ & - \tfrac{1}{16}\chi^6\langle\cos^6\theta_{12}\rangle_{\Omega_1,\Omega_2} - \tfrac{5}{128}\chi^8\langle\cos^8\theta_{12}\rangle_{\Omega_1,\Omega_2}\ldots).\end{aligned} \tag{13}$$

Substituting equation (13) in the pressure equation, one gets

$$\frac{\beta p_0}{\varrho} = 1 + \frac{2\eta(2 - \eta)}{(1 - \eta)^3}[F_0(\chi) - F_2(\chi)S_2^2 - F_4(\chi)S_4^2], \tag{14}$$

where $\eta(=\varrho V_0)$ is the packing fraction and

$$S_n = \int f(\Omega)P_n(\cos\theta)\, d\Omega, \tag{15}$$

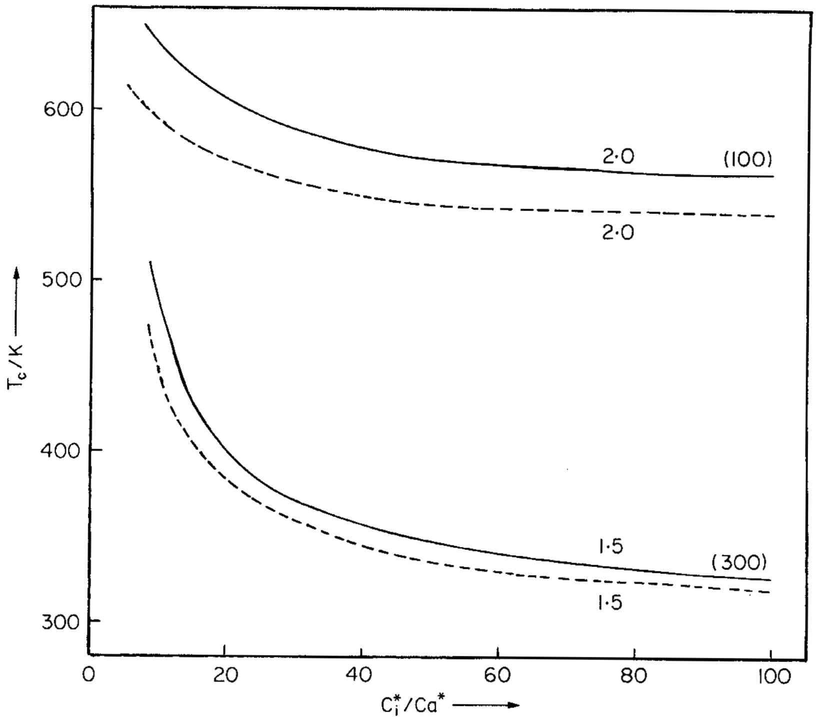

Figure 2. The variation of N–I transition temperature T_c as a function of C_i^*/C_a^* for a fixed value of C_i^*/k = 4000·0 (K). The numbers on curves indicate the value of x_0. Dashed lines correspond to pressure 1 bar and the numbers in parentheses on the solid lines indicate the pressure in bars.

$$F_0(\chi) = (1-\chi^2)^{-1/2}[1 - \tfrac{1}{6}\chi^2 - \tfrac{1}{40}\chi^4 - \tfrac{1}{112}\chi^6 - \ldots], \tag{16}$$

$$F_2(\chi) = \tfrac{1}{3}(1-\chi^2)^{-1/2}[1 + \tfrac{3}{14}\chi^2 + \tfrac{5}{56}\chi^4 + \tfrac{25}{528}\chi^6 + \ldots], \tag{17}$$

$$F_4(\chi) = \tfrac{1}{35}(1-\chi^2)^{-1/2}[1 + \tfrac{15}{22}\chi^2 + \tfrac{525}{1184}\chi^4 + \ldots]. \tag{18}$$

The Helmholtz free energy per particle for the reference system can be obtained from equation (14)

$$\frac{\beta A_0}{N} = (\ln\varrho - 1) + \langle \ln[4\pi f(\Omega)] \rangle + \frac{\eta(4-3\eta)}{(1-\eta)^2}[F_0(\chi) - F_2(\chi)S_2^2 - F_4(\chi)S_4^2], \tag{19}$$

where the first two terms represent the free energy of a gas of non-interacting rods. Other thermodynamic quantities can be obtained by using equation (5) and equation (19) and standard thermodynamic relations.

2.2. *First-order perturbation*

The Helmholtz free energy in the first-order perturbation is given by

$$\frac{\beta A^{(1)}}{N} = \beta \int d\Omega_1 F(\Omega_1)\psi^{(1)}(\Omega_1), \tag{20}$$

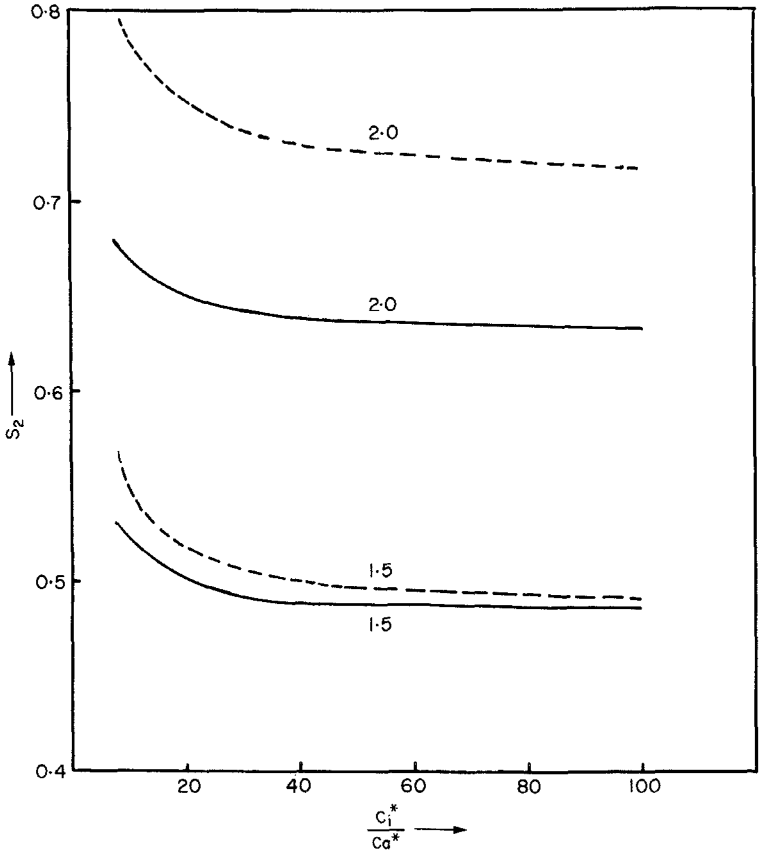

Figure 3. The variation of order parameter S_2 at the N–I transition as a function of C_i^*/C_a^*. C_i^*/k is chosen so as to reproduce $T_c = 409$ (K). The numbers on the curves indicate the value of x_0. Line symbols are the same as for figure 1.

where

$$\psi^{(1)}(\Omega_1) = \tfrac{1}{2}\varrho \int d\Omega_2 f(\Omega_2) \int d\mathbf{r}_{12} u_p(\mathbf{r}_{12}, \Omega_1, \Omega_2) \tilde{g}^{(0)}(\mathbf{r}_{12}, \Omega_{12}). \tag{21}$$

We adopt the following form for the perturbation potential

$$u_p(\mathbf{r}_{12}, \Omega_1, \Omega_2) = -\frac{C_i}{r_{12}^6} - \frac{C_a}{r_{12}^6} P_2(\cos\theta_{12}); \quad \text{for } r_{12} > D(\Omega_{12}), \tag{22}$$

where C_i and C_a are constants related to the isotropic and anisotropic dispersion interaction and θ_{12} is the angle between the long axes of the two molecules. This is certainly a drastic oversimplification of the intermolecular potential of real liquid crystals but this is in accord with the Maier–Saupe theory [15].

Following the algebra given in I and using the decoupling approximation, we can express equation (22) as

$$\psi^{(1)}(\cos\theta_1) = -\phi_0 - \phi_2 S_2 P_2(\cos\theta_{12}) - \phi_4 S_4 P_4(\cos\theta_{12}), \tag{23}$$

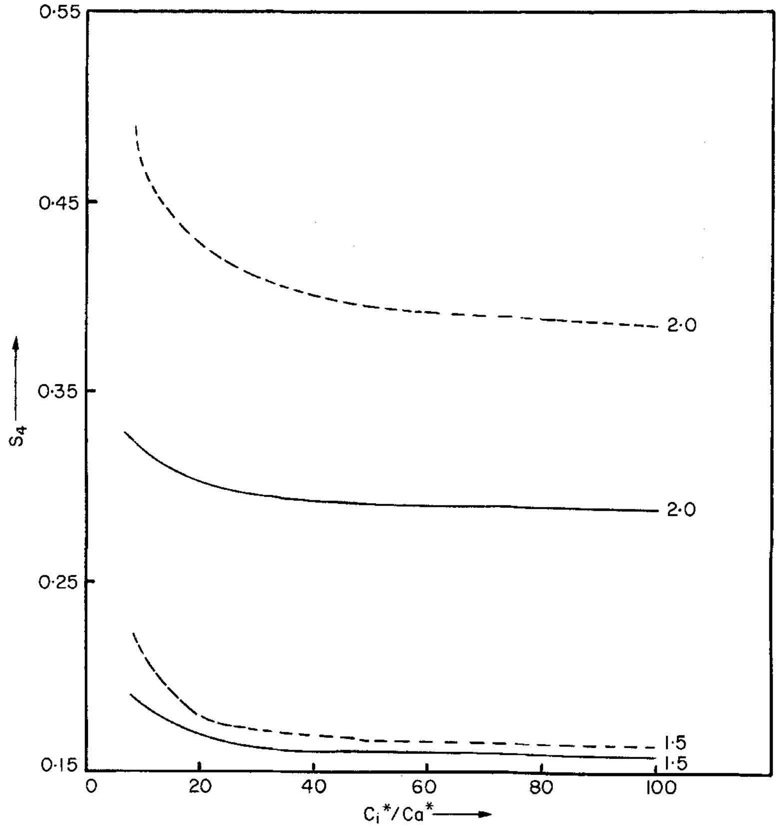

Figure 4. The variation of order parameter S_4 at the N–I transition as a function of C_i^*/C_a^*. C_i^*/k is chosen so as to reproduce $T_c = 409$ (K). The numbers on the curves indicate the value of x_0. Line symbols are the same as for figure 1.

where

$$\phi_0 = \tfrac{1}{12}\pi\eta I_6(\eta)x_0C_i^*\left(A_0 + \frac{1}{5}\frac{C_a^*}{C_i^*}A_2\right), \tag{24}$$

$$\phi_2 = \tfrac{1}{12}\pi\eta I_6(\eta)x_0C_i^*\left[A_2 + (A_0 + \tfrac{2}{7}A_2 + \tfrac{2}{7}A_4)\frac{C_a^*}{C_i^*}\right], \tag{25}$$

$$\phi_4 = \tfrac{1}{12}\pi\eta i_6(\eta)x_0C_i^*\left[A_4 + [(\tfrac{18}{35}A_2 + \tfrac{20}{27}A_4)]\frac{C_a^*}{C_i^*}\right], \tag{26}$$

with $C_i^* = C_i/V_0^2$, and the values of the constants A_n as a function of length-to-width ratio x_0 are tabulated in I for several values of n. The integral I_6, defined as

$$I_6(\varrho, T) = \int_0^\infty r_{12}^{*-4}g_{\rm hs}^{(0)}(r_{12}^*)\,dr_{12}^*, \tag{27}$$

can be obtained by knowing the exact radial distribution function for hard spheres obtained from computer simulation. Larsen *et al.* [14] found the following series for I_6:

$$I_6(\eta) = 0.3333 + 0.429911\eta + 0.24182\eta^2 + 0.0176\eta^3 + 0.0908\eta^4 - 0.1711\eta^5. \tag{28}$$

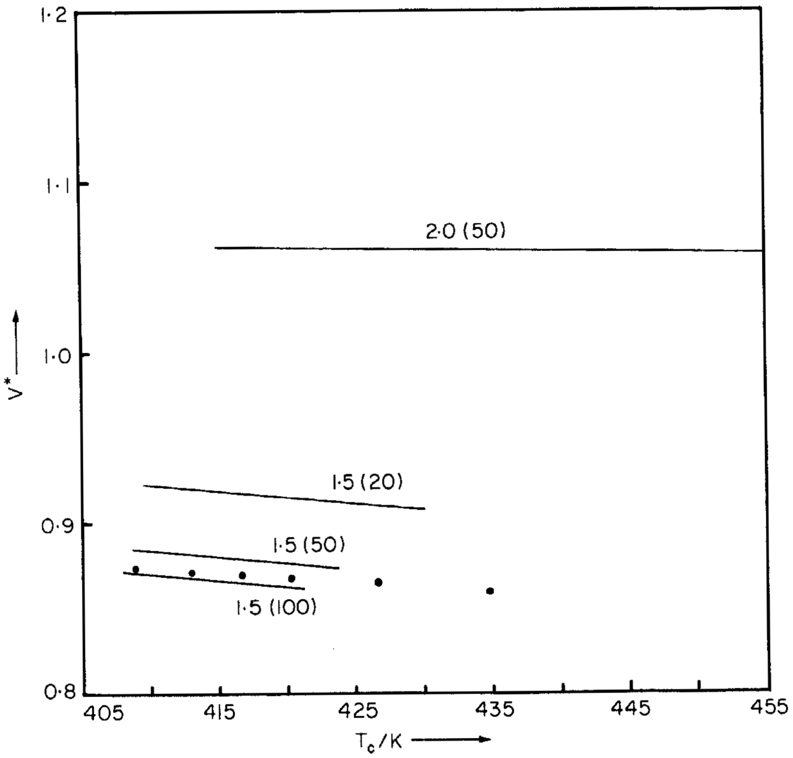

Figure 5. The variation of reduced volume $V^*(=\pi/6\eta)$ at the NI transition as a function of transition temperature T_c. The numbers on the curves with and without parentheses indicate, respectively, the values of C_i^*/C_a^* and x_0. The parameter C_i^*/k is chosen so as to reproduce the transition temperature $T_c = 409$ (K) at $P = 1$ bar. Experimental points for PAA are taken from [6].

ϕ_0, ϕ_2 and ϕ_4 and ϕ_4/ϕ_2 were tabulated in I as a function of packing fraction η and length-to-width ratio x_0. It was found that the contribution of ϕ_4 increase with x_0. For $x_0 \geqslant 2$, the contribution of higher-order terms are quite substantial.

With the help of equations (20) and (23) the first order correction to the free energy is given by

$$\frac{\beta A^{(1)}}{N} = -\beta\phi_0 - \beta\phi_2 S_2^2 - \beta\phi_4 S_4^2. \qquad (29)$$

The first-order correction to the compressibility factor is found to be

$$\frac{\beta p^{(1)}}{\varrho} = \beta t_0 + \beta t_2 S_2^2 + \beta t_4 S_4^2, \qquad (30)$$

where

$$t_0 = L\left(A_0 + \frac{1}{5}\frac{C_a^*}{C_i^*}A_2\right), \qquad (31)$$

$$t_2 = L\left[A_2 + (A_0 + \tfrac{2}{7}A_2 + \tfrac{2}{7}A_4)\frac{C_a{}^*}{C_i^*}\right], \qquad (32)$$

$$t_4 = L\left[A_4 + (\tfrac{18}{35}A_2 + \tfrac{20}{77}A_4)\frac{C_a^*}{C_i^*}\right], \qquad (33)$$

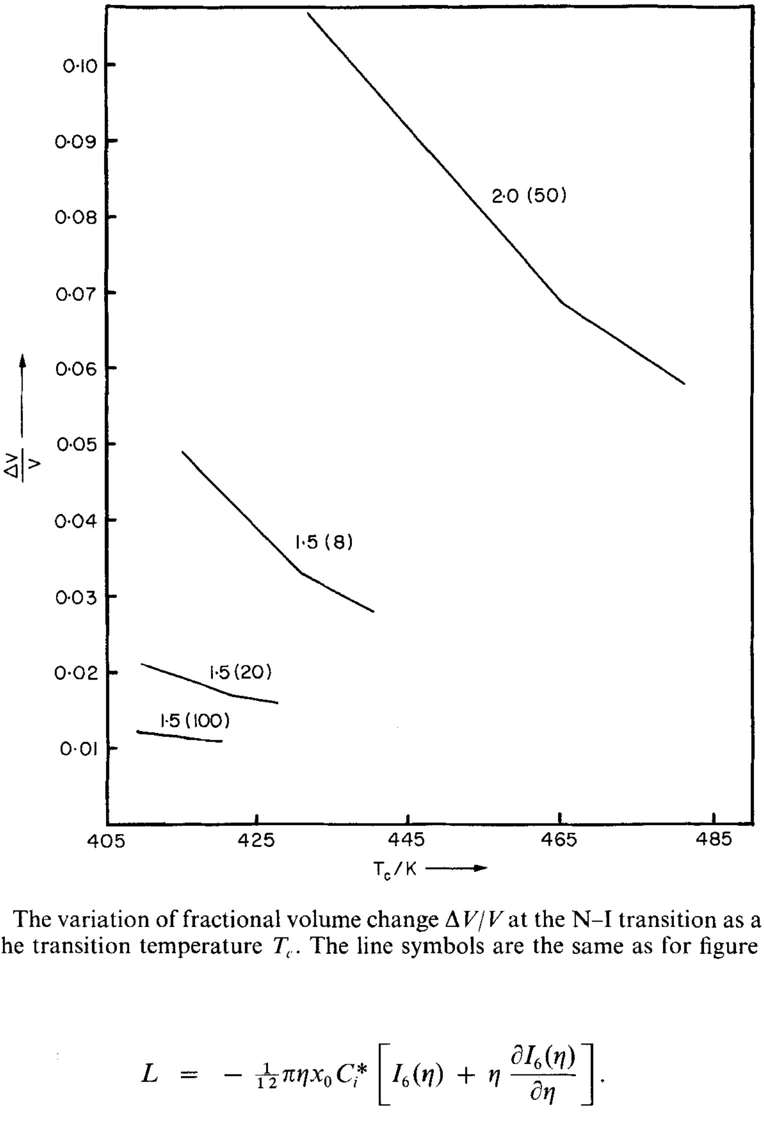

Figure 6. The variation of fractional volume change $\Delta V/V$ at the N–I transition as a function of the transition temperature T_c. The line symbols are the same as for figure 5.

with

$$L = -\tfrac{1}{12}\pi\eta x_0 C_i^* \left[I_6(\eta) + \eta \frac{\partial I_6(\eta)}{\partial \eta} \right]. \tag{34}$$

2.3. *Conditions for thermodynamic equilibrium*

The total configurational Helmholtz free energy can be written as

$$\frac{\beta A}{N} = \frac{\beta A_0}{N} + \frac{\beta A^{(1)}}{N}. \tag{35}$$

Substituting $\beta A_0/N$ and $\beta A^{(1)}/N$, we get

$$\frac{\beta A}{N} = \langle [\ln 4\pi f(\Omega)] \rangle + C_2 - B_2 S_2^2 - B_4 S_4^2, \tag{36}$$

where

$$C_2 = (\ln \varrho - 1) + \frac{\eta(4 - 3\eta)}{(1 - \eta)^2} F_0(\chi) - \beta\phi_0, \tag{37}$$

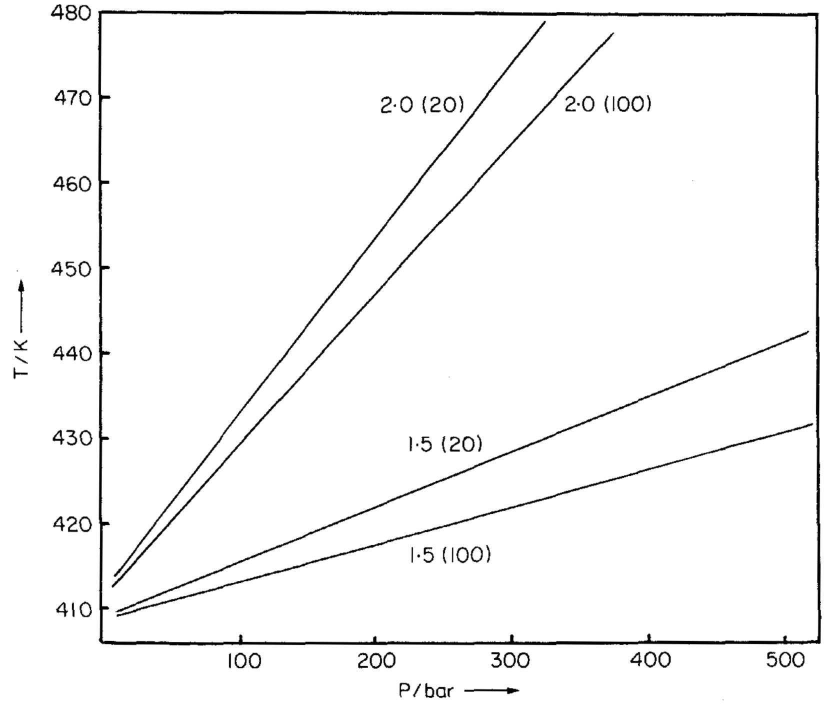

Figure 7. The variation of temperature with pressure for different values of x_0 and C_i^*/C_a^* at constant density. The line symbols are the same as for figure 5.

$$B_2 = \frac{\eta(4-3\eta)}{(1-\eta)^2} F_2(\chi) + \beta\phi_2, \tag{38}$$

$$B_4 = \frac{\eta(4-3\eta)}{(1-\eta)^2} F_4(\chi) + \beta\phi_4. \tag{39}$$

The compressibility factor is given by

$$\frac{\beta p}{\varrho} = \frac{\beta p_0}{\varrho} + \frac{\beta p^{(1)}}{\varrho}, \tag{40}$$

$$= 1 + \left[\frac{2\eta(2-\eta)}{(1-\eta)^3} F_0(\chi) + \beta t_0\right] + \left[\beta t_2 - F_2(\chi)\frac{2\eta(2-\eta)}{(1-\eta)^3}\right] S_2^2$$
$$+ \left[\beta t_4 - \frac{2\eta(2-\eta)}{(1-\eta)^3} F_4(\chi)\right] S_4^2. \tag{41}$$

The minimization of the free energy with respect to variations in $f(\Omega)$ subject to the constraint $\int f(\Omega) d\Omega = 1$ determines the one-particle orientational distribution at a fixed temperature and pressure. Thus the form of $f(\Omega)$ is obtained from equation (36); i.e.

$$f(\Omega) = \frac{\exp[2B_2S_2P_2(\cos\theta) + 2B_4S_4P_4(\cos\theta)]}{\int \exp[2B_2S_2P_2(\cos\theta) + 2B_4S_4P_4(\cos\theta)]}, \tag{42}$$

The nematic–isotropic transition parameters under high pressure. S_2 and S_4 are the order parameters, $\Delta\Sigma/Nk$ the transition entropy; $\Gamma(T_c)$ is defined in equation (47). The model parameters are chosen so as to reproduce transition temperature T_c = 409 K at P = 1 bar, $V^* = \pi/6\eta$ and $\Delta V/V$ is the fractional change in volume.

x_0	C_i^*/k	C_i^*/C_a^*	P (par)	T_c	V^*	$\Delta V/V$	S_2	S_4	$\Delta\Sigma/Nk$	Γ (T_c)	(dT_c/dP)
1·5	3458·5242	8	10	410·10	1·0039	0·0490	0·5684	0·2206	1·3760	1·9470	119·85
			100	420·48	0·9964	0·0400	0·5522	0·2074	1·2239	1·9668	108·03
			200	430·89	0·9880	0·0334	0·5390	0·1971	1·1103	1·9880	97·82
			300	440·39	0·9800	0·0288	0·5294	0·1897	1·0301	2·0092	89·73
	4295·3472	20	10	409·60	0·9235	0·0211	0·5140	0·1785	0·9535	2·178	66·51
			100	415·50	0·9184	0·0192	0·5091	0·1749	0·9113	2·197	62·69
			200	421·67	0·9132	0·0174	0·5046	0·1717	0·8735	2·219	59·06
			300	427·50	0·9083	0·0160	0·5009	0·1691	0·8426	2·239	55·93
	4885·9538	50	10	409·45	0·8842	0·0143	0·4974	0·1668	0·8305	2·351	49·05
			100	413·83	0·8807	0·0134	0·4948	0·1654	0·8081	2·370	47·00
			200	418·50	0·8769	0·0125	0·4924	0·1633	0·7866	2·390	44·98
			300	422·89	0·8734	0·0118	0·4902	0·1618	0·7682	2·410	43·18
	5146·0712	100	10	409·41	0·8701	0·0124	0·4926	0·1636	0·7937	2·429	43·75
			100	413·33	0·8670	0·0117	0·4906	0·1622	0·7759	2·448	42·15
			200	417·52	0·8638	0·0111	0·4887	0·1608	0·7586	2·469	40·54
			300	421·17	0·8602	0·0105	0·4861	0·1592	0·7416	2·492	38·93
2·00	2864·9486	20	300	472·31	1·0788	0·0775	0·6477	0·3023	1·637	2·588	176·14
			400	489·56	1·0758	0·0621	0·6287	0·2852	1·415	2·646	158·31
			500	505·67	1·0716	0·0598	0·6130	0·2723	1·397	2·710	142·99
	3000·6398	50	300	465·40	1·0584	0·0684	0·6369	0·2915	1·5452	2·7104	160·03
			400	481·01	1·0523	0·0579	0·6203	0·2749	1·3879	2·7660	148·50
			500	495·58	1·0457	0·0505	0·6074	0·2625	1·2737	2·8220	139·04
	3052·0726	100	300	463·11	1·0509	0·0654	0·6331	0·2878	1·513	2·758	154·54
			400	478·21	1·0449	0·0557	0·6174	0·2723	1·365	2·815	143·73
			500	492·32	1·0387	0·0487	0·6051	0·2604	1·256	2·872	134·88

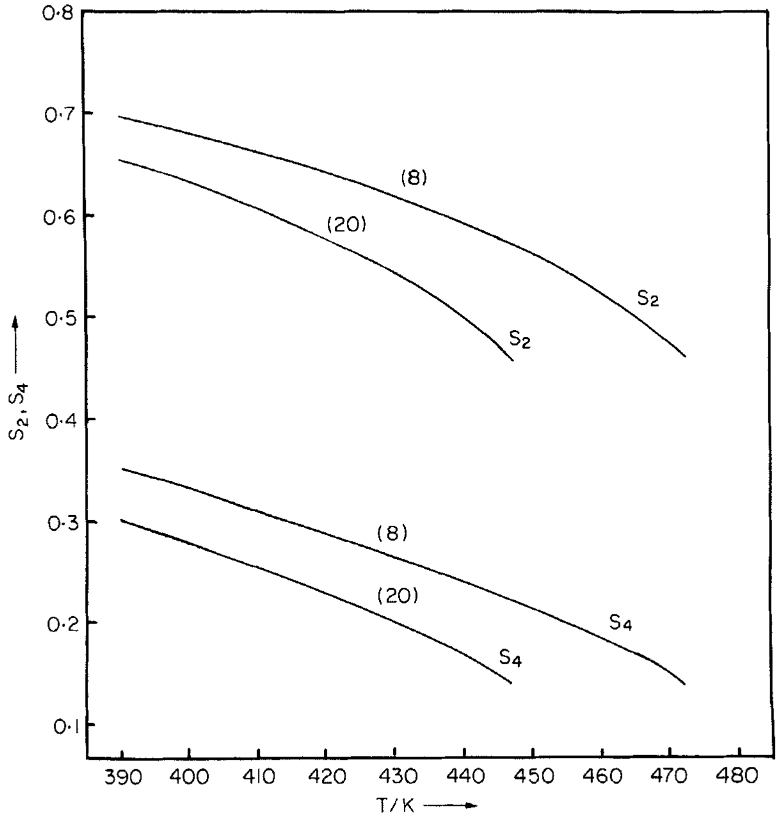

Figure 8. The variation of order parameters S_2 and S_4 as a function of temperature at fixed densities for $x_0 = 1{\cdot}5$. Numbers on the curves indicate the ratio $C_i^*/C_a^*(C_i^*/k = 3458{\cdot}5242$ for $C_i^*/C_a^* = 8$ and $C_i^*/k = 4295{\cdot}3472$ for $C_i^*/C_a^* = 20)$.

which leads directly to the transcendental equations for the second- and fourth-rank order parameters as defined by

$$S_2 = \int d\Omega f(\Omega) P_2(\cos\theta), \tag{43}$$

and

$$S_4 = \int d\Omega f(\Omega) P_4(\cos\theta). \tag{44}$$

The nematic–isotropic transition at constant pressure is located by equating the pressure and chemical potentials of the two phases,

$$\left.\begin{aligned} p_{\text{nem}}(\eta_{nc}, T_c, S_{2c}, S_{4c}) &= p_{\text{iso}}(\eta_{ic}, T_c), \\ \mu_{\text{nem}}(\eta_{nc}, T_c, S_{2c}, S_{4c}) &= \mu_{\text{iso}}(\eta_{ic}, T_c). \end{aligned}\right\} \tag{45}$$

S_{2c} and S_{4c} are determined from equations (43) and (44). Keeping the pressure fixed, we get five equations involving five unknowns η_{nc}, η_{ic}, T_c, S_{2c} and S_{4c}. We solve them numerically by an iterative procedure.

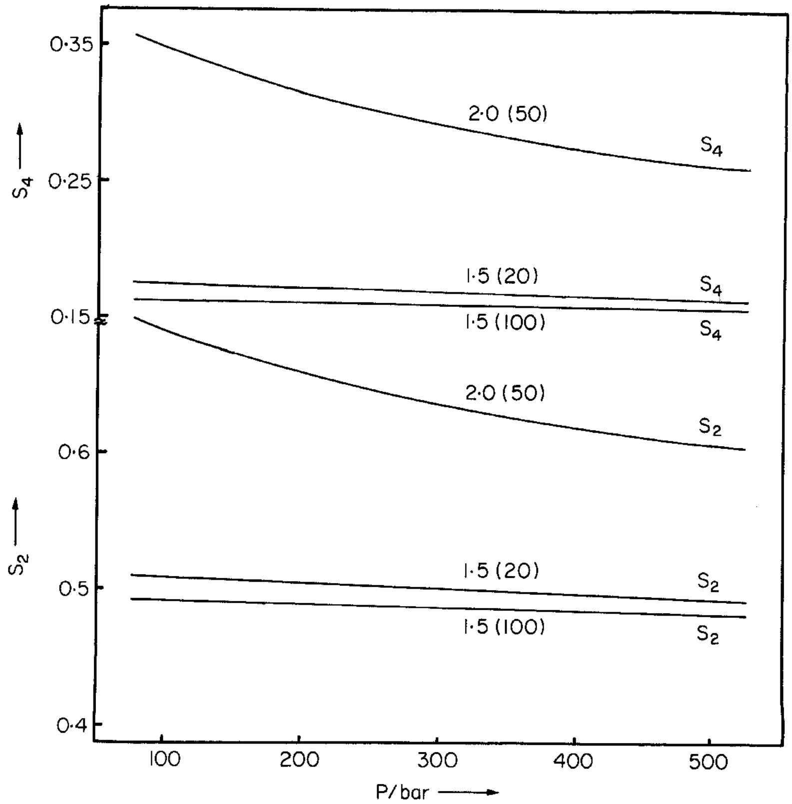

Figure 9. The variation of order parameters S_2 and S_4 as a function of pressure at fixed C_i^*/k.

3. Results and discussion

We have used the following values for the interaction parameters and the molecular volume

$$\left.\begin{aligned} C_i^*/k &= 4000\,\mathrm{K}, \\ C_a^*/C_i^* &= 1/20 \text{ and } 1/50 \\ V_0 &= 230\,\text{Å}^3. \end{aligned}\right\} \tag{46}$$

and

The values of the force parameters and V_0 taken here approximately correspond to those used in the calculation of the nematic–isotropic transition of PAA by several workers. The values of V_0 for PAA was estimated by Viellard-Baron [16] using van der Waals radii and bond lengths from crystallographic data. The value of C_i is estimated from the latent heat of vaporization [17]. We first investigate the effects caused by ellipsoidal hard core length-to-width ratio x_0 and the potential parameters C_i and C_a as defined by equation (22) on the thermodynamic properties close to NI phase transition as a function of pressure. Using equation (45), NI transition parameters are determined at various constant values of pressure ranging from 1 bar to 500 bar. The method of calculation is similar to that given in I.

Figure 1 is a plot of the variation of transition temperature T_c with the interaction strength parameter C_i^*/k corresponding to pressures of 1 bar and 300 bar for x_0 equal to 1·5 and 2·0. The variation of T_c and of the order parameter S_2 with the ratio C_i^*/C_a^* are shown, respectively, in figure 2 and figure 3 for a fixed value of C_i^*/k corresponding to pressures 1 bar and 300 bar for $x_0 = 1{\cdot}5$ and 1 bar and 100 bar for $x_0 = 2{\cdot}0$. Figure 4 is a plot of the fourth-rank order parameter S_4 at the NI transition as a function of C_i^*/C_a^* and corresponding to pressures 1 bar and 300 bar for $x_0 = 1{\cdot}5$ and 1 bar and 100 bar for $x_0 = 2{\cdot}0$. C_i^*/k is chosen so as to reproduce $T_c = 409\,\mathrm{K}$. We observe a jump in S_4 with increasing pressure at fixed x_0. It can also be seen from the figure that for a given x_0 for $C_i^*/C_a^* > 20$, the S_4 value is not very sensitive to this ratio.

We have summarized a number of thermodynamic properties at the NI transition in the table. For a given x_0 and C_i^*/C_a^*, the parameter C_i^*/k was chosen so as to reproduce quantitatively the transition temperature $T_c = 409\,\mathrm{K}$ at $p = 1$ bar. Comparing the results listed in the table with the corresponding results obtained in II, we find that inclusion of S_4 terms in the calculation leads to a slight change in thermodynamic quantities. The order parameter S_2, relative volume change $\Delta V/V$ and transition entropy $\Delta\Sigma/Nk$ (measure of the change in entropy at the transition) increase whereas the reduced volume V^* $(=\pi/6n)$ decreases slightly. The parameter Γ listed in the table and defined as

$$\Gamma = \frac{V\,(\partial S/\partial V)_T}{T\,(\partial S/\partial T)_V} = \left(\frac{\partial \ln T}{\partial \ln \varrho}\right)_S \tag{47}$$

measures the relative sensitivity of the order parameter to volume change and temperature change. The pressure dependence of the transition temperature (dT_c/dP) is determined by Clausius-Clapeyron's law. Γ and (dT_c/dP) both increase very slightly due to S_4. As x_0 is increased in II as well as in the present work, the values of S_2, S_4, V^*, $\Delta V/V$, $\Delta\Sigma/Nk$, dT_c/dP and Γ go up.

Figures 5, 6, and 7 show, respectively, the variation of reduced volume V^* and $\Delta V/V$ with T_c and transition temperature T_c with pressure at a fixed C_i^*/k. The trends in these figures are qualitatively identical to those presented in II.

In figure 8 we have plotted second- and fourth-rank long-range orientational order parameters (S_2, S_4) as a function of temperature at fixed density for $x_0 = 1{\cdot}5$. The values are obtained by starting at $p = 1$ bar and a temperature of about 390 K; the temperature is then raised while keeping density fixed as in the experiment of McColl and Shih [18]. In accordance with the experimental result [18] we find that transition occurs at higher temperature compared to the case when the temperature is raised at constant pressure. In figure 9 we have plotted S_2 and S_4 as a function of pressure at fixed C_i^*/k. The decrease in S_2 and S_4 at the transition with an increase in pressure is in accordance with the experimental results by Horn and Faber [2].

The general trends in the transition quantities in the present work are identical with those presented and discussed in II. Inclusion of the fourth-rank order parameter S_4 in the calculation does not lead to a significant overall improvement. Quantitative agreement between theory and experiment cannot really be expected as our model system crudely simulates a real system.

Though the decoupling approximation introduces anisotropy in the pair concentration function (PCF) and is exact at very low density, it cannot be exact at liquid density. It can be easily seen that when two molecules are parallel, the PCF is most anisotropic and when $\hat{\mathbf{e}}_1 \perp \hat{\mathbf{e}}_2$, it is most isotropic. It therefore seems that the decoupling approximation overemphasizes the anisotropy in the pair correlation function for the parallel configuration and underestimates that for perpendicular configurations. The decoupling approximation has, however, been found to yield values of the compressibility factor in good agreement with computer simulation results [19, 20]. This justifies the use of decoupling approximations for a system of hard ellipsoids.

We are grateful to U.G.C. New Delhi, for the award of a minor research grant.

References

[1] Frenkel, D., and Mulder, B. M., 1985, *Molec. Phys.*, **55**, 1171. Frenkel, D., 1987, *Molec. Phys.*, **60**, 1.
[2] Horn, R. G., and Faber, T. E., 1979, *Proc. R. Soc.* A, **368**, 199.
[3] Keyes, P. H., and Daniels, W. B., 1979, *J. Phys., Paris*, **40**, C3, 380.
[4] Emsley, J. W., Luckhurst, G. R., and Timimi, B. A., 1982, *Molec. Phys.*, **44**, 659.
[5] Pollman, P., and Scherer, G., 1980, *Ber. Bunsenges. phys. Chem.*, **84**, 57.
[6] Tranfield, R. V., and Collings, P. J., 1982, *Phys. Rev.* A, **25**, 2744.
[7] Savithramma, K. L., and Madhusudana, N. V., 1983, *Molec. Crystals liq. Crystals*, **97**, 407.
[8] Singh, S., and Singh, Y., 1982, *Molec. Crystals liq. Crystals*, **87**, 211, referred to in the text as I.
[9] Singh, S., and Singh, K., 1983, *Molec. Crystals liq. Crystals*, **101**, 77, referred to in the text as II.
[10] Singh, K., and Singh, S., 1984, *Molec. Crystals liq. Crystals*, **108**, 133.
[11] Kachinskii, V. N., Ivanov, V. A., Zisman, A. N., and Stishov, S. M., 1979, *J. exp. theor. Phys.*, **48**, 273.
[12] Berne, B. J., and Pechukas, P., 1972, *J. chem. Phys.*, **56**, 4213.
[13] Parsons, J. D., 1979, *Phys. Rev.* A, **19**, 1225.
[14] Larsen, B., Rasaiah, J. C., and Stell, G., 1977, *Molec. Phys.*, **133**, 987.
[15] Maier, W., and Saupe, A., 1959, (*a*), *Z. Naturf.*, **14**, 882; 1960, *Ibid.*, **15**, 287.
[16] Viellard-Baron, J., 1974, *Molec. Phys.*, **28**, 809.
[17] Solsky, J., and Gurushka, E., 1974, *J. phys. Chem.*, **78**, 275.
[18] Mc Coll, J. R., and Shih, C. S., 1972, *Phys. Rev. Lett.*, **29**, 86.
[19] Singh, U. P., and Singh, Y., 1986, *Phys. Rev.* A, **33**, 2725.
[20] Frenkel, D., Mulder, B. M., and MacTague, 1984, *Phys. Rev. Lett.*, **52**, 287.